Modeling of Ion-Exclusion and Vacancy Ion-Exclusion Chromatography in Analytical and Concentration Overload Conditions

Krzysztof Kaczmarski[1,*], Wojciech Zapała[1], Wojciech Wanat[1], Masanobu Mori[2], Bronisław K. Głód[3], and **Teresa Kowalska[4]**

[1]Faculty of Chemistry, Technical University of Rzeszów, Al Powstanców Warszawy 6, 35-959 Rzeszów, Poland; [2]National Institute of Advanced Industrial Science and Technology at Seto, 110, Nishiibara-cho, Seto, 489-0884, Japan; [3]Meat and Fat Research Institute, Jubilerska 4, 04-190 Warsaw, Poland; and [4]Institute of Chemistry, Silesian University, 9 Szkolna Street, 40-006 Katowice, Poland

Abstract

Ion-exclusion chromatography (IEC) finds applications in various different analytical separations of weak acids. Pure, deionized water or a diluted, aqueous solution of a strong mineral acid (such as, e.g., sulphuric acid) is used as the mobile phase, whereas a typical stationary phase is a strongly acidic resin in the H^+ form (e.g., the sulfonated polystyrene–divinylbenzene resin with a high ion-exchange capacity, provided by the sulfonic acid groups). When pure water is used as the mobile phase, then the characteristic leading (i.e., frontally tailing) peaks are obtained, and the retention depends mainly on the concentration of the analyte. An alternative technique is vacancy ion-exclusion chromatography (v-IEC), in which the column is equilibrated with the sample solution, flowing as the mobile phase through the system, and pure water is injected as the sample. In this case, the symmetrical vacant peaks are obtained. The aim of this paper is to describe the retention mechanism in IEC and v-IEC for the adsorptive and nonadsorptive acids in analytical and concentration overload conditions, with pure water and the diluted sulphuric acid solution as the two different mobile phases. The retention times and the peak shapes predicted by the derived equations remain in a good qualitative and quantitative agreement with the experimental data. The model proposed in this paper predicts the new features characteristic of IEC for the adsorptive acids. These are, namely, an increase in the retention time of the peak apexes (up to a certain level and concurring with an increase in the acid concentration), followed by a subsequent decrease of the retention time (with the further growth of the acid concentration in the eluent). Similar changes in the retention time observed for v-IEC in the specific adsorption conditions were also correctly predicted by the model.

Introduction

Ion-exclusion chromatography (IEC) is a chromatographic technique applied to the separation of partially ionized molecules (1–5). When the pure ion exclusion mechanism of retention is involved, the retention volumes of the medium-strength electrolytes are proportional to the values of their respective dissociation constants (pK_a). The strong ($pK_a < 2.5$) and weak ($pK_a > 6.5$) electrolytes are eluted without separation, with the former group at the beginning and the latter one at the end of the elution order (6).

Similar to other chromatographic techniques, the notion of IEC is derived from the predominant mechanism of retention, which is ion exclusion. Yet, electrostatic repulsion is not the sole factor that determines the retention time, and frequently, the side effect of IEC (i.e., hydrophobic adsorption) has to be taken into account as well. For this particular reason, some authors refer to this technique as IEC/adsorption chromatography.

A characteristic feature of IEC is an equal charge of both the dissociated functional groups of the ion-exchange resin and of the analyte itself. Hence, the negatively charged ions (e.g., the dissociated acidic compounds) are separated on the highly acidic cation-exchange resins in the H^+ form, with the anionic functional groups [such as, e.g., the sulfonic acid functionalities, (SO^{3-})] fixed to the resin matrix. Although a column of this type can equally be used for IEC and ion-exchange chromatography, the real ion-exchange reactions are not involved in the IEC mechanism. For the specific requirements of IEC, a high ion-exchange capacity (e.g., of the magnitude order equal to ca. 1.5 mequiv/mL) is preferred. Water molecules occlude as hydration spheres around the dissociated functional groups of the support. Contained in the resin pores and in the hydration spheres, they are immobilized, forming a stationary phase. Neutral, uncharged molecules penetrate into the resin, as the similarly charged co-ions are repulsed (excluded) by the presence of the dissociated functional groups, immobilized in the resin skeleton.

Dilute aqueous solutions of sulphuric acid are most frequently used as mobile phases in IEC. A small addition of this mineral acid prevents the peaks from tailing, which is a commonly

*Author to whom correspondence should be addressed: email kkaczmarski@prz.edu.pl.

observed negative phenomenon when pure deionized water is used as the eluent. Peak fronting results from an obvious lack of the buffer capacity with an aqueous eluent, and for this reason, the pH of the eluent should be maintained constant. An increased proton concentration suppresses the ionization of the sample acids, allowing high-performance separations by an improvement of the peak shape and of the detection sensitivity. Therefore, the pH value of the mobile phase is an important factor that influences the retention time of the peaks and the resolution quality in IEC (7).

Another method to avoid the peak tailing is to employ the v-IEC. In this case, a mixture of the analytes is used as the mobile phase and pure water is tested as a sample (8–12). As a result, the characteristic negative "vacant" peaks (elution dip peaks) are obtained. Similar to IEC, and also with v-IEC, the main retention mechanism (based on the exclusion of ions) can be coupled with a complementary adsorption of an analyte on the resin phase.

The main factors that influence retention in the v-IEC mode include characteristics (such as ionization and hydrophobicity), the concentration of the sample acids in the eluent, the pH of mobile phase (buffered to maintain a constant ionization degree, pK_a), and the presence of an organic modifier (such as, e.g., aliphatic alcohols, sugars, or acetonitrile) in an injected water sample (13). An increased concentration of the analytes in the eluent elongates the retention time, as the more diluted acids dissociate better and are eluted faster than the acids in the molecular form (14). The temperature increase was found as an almost negligible factor because, with higher acids (longer carbon chain aliphatic acids), it induced a slight decrease in the retention time only. It is important to note, that with higher acids adsorption plays a complementary, yet measurable role in their retention mechanism (15).

The attempts to model the retention mechanism for the IEC and v-IEC modes can already be found in the literature. A good qualitative agreement between the experimental and the theoretical peak profiles was obtained when the Craig model was employed for the description of the single acid retention by means of IEC (16,17). However, in those two papers, the dependency of the retention times on the acid concentration was not analyzed. In the literature (18), the equilibrium-dispersive model (19) was successfully applied to the analysis of retention in the IEC and v-IEC modes of single acids with pure water as the eluent. The analysis was performed for the acids whose adsorption could be neglected. In that case, a good quantitative agreement was obtained between the experimental and the theoretical retention times for the different sample concentrations.

The aim of this paper was to model the retention mechanism in the IEC and v-IEC modes for analytical and concentration overload conditions, with the nonadsorptive and adsorptive acids in both cases (i.e., when pure water and the water plus a small addition of the strong mineral acid are employed as the mobile phase). To obtain this goal, the Craig model, coupled with the equilibrium relationship between the acids and their ions and implemented with an appropriate isotherm model, was used. The further part of presented discussion focuses on the modeling of separation with the multi-component solutions of organic acids.

Theory

Retention of acids in IEC for diluted solutions

There are two kinds of models utilized for description of chromatographic separation: (*i*) The mass transfer models (19,20) and (*ii*) the Craig cell model (21). The most complicated among the first category of the models was the general rate model, in which the mass transfer resistances and the axial dispersion were explicitly taken into account. In the simplest mass transfer model (i.e., in the equilibrium dispersive model), the mass transfer resistances and the dispersion effects were lumped into one apparent dispersion coefficient (D_a) and were considered implicitly. In practice, the dispersion coefficient is calculated from a measured number of theoretical plates (19). Alternatively, in the Craig model, the column is divided into the perfectly mixed cells. It was assumed that in each cell the equilibrium between the species in the mobile and stationary phases were established immediately at each individual time step of the model integration. The cell number was chosen in such a way as to simulate the apparent dispersion in the column. The advantage of the mass transfer model was the ease of analyzing the separation process with the real values of the mass transfer coefficient and the dispersion coefficient for each individual component, which was impossible with the Craig model. However, the time of computational solution of the mass transfer model considerably increased when it had to be solved with an implicate isotherm model (22) or with the non-linear relationship between the ionized and the non-ionized forms of acidic or basic compounds in IEC (18). Contrary to the mass transfer model, the Craig model proved effective in the computer simulation of the acid retention (16,17). Because the analysis of the impact of mass transfer resistance exerted on the IEC and the v-IEC separations remained beyond the scope of the present work, the Craig method was selected for modeling the chromatographic processes.

The Craig model of IEC and v-IEC

In the Craig model, the column is divided into a number of equal cells. The following denotations were used: the geometrical volume of the cell was V_c; the volume of the eluent contained among the adsorbent particles in the cell was V_e; the volume of the pores inside the adsorbent particles was V_p; and the total volume of the eluent in the cell was $V_t = V_e + V_p$.

The Craig model assumed that the volume (V_e) of the eluent with the non-dissociated (HR) and the dissociated (R^-) form of the acid flows from the cell *i-1* to the cell *i* in the time $t - \Delta t$, and it mixes with the eluent occluded in the adsorbent pores V_p of the *i*-th cell in the time $t - \Delta t$. After the time (Δt), the new equilibrium between the ions (R^-) and the non-dissociated acid molecules (HR) in the eluent and non-dissociated adsorbed and non-adsorbed acid molecules is established. Moreover, it was assumed that the mass transfer resistances could be neglected and that the functional groups did not modify water inside the adsorbent particles (V_P). Thus, that the concentration of the non-dissociated acid in the eluent occluded in the pores was the same as in the bulk mobile phase. Furthermore, it was assumed that only the non-dissociated acid molecules can adsorb on the adsorbent surface, although the respective ions can penetrate inside

the stationary phase pores (V_P).

Under the described assumptions, the mass balance for the non-dissociated acid (HR) and for the dissociated ions (R^-) can be given as:

$$V_e \cdot C^{j,HR}_{e,i-1,t-\Delta t} + V_e \cdot C^{j,R^-}_{e,i-1,t-\Delta t} + V_p \cdot C^{j,HR}_{p,i,t-\Delta t} + V_p \cdot C^{j,R^-}_{p,i,t-\Delta t} + (V_c - V_t) q^{j,HR}_{i,t-\Delta t} + (V_c - V_t) q^{j,HR}_{i,t} = (V_e + V_p) C^{j,HR}_{i,t} + C^{j,R^-}_{e,i,t} \cdot V_e + V_p \cdot C^{j,R^-}_{p,i,t} \quad \text{Eq. 1}$$

where j denotes the *j-th* component ($j = 1,2, \ldots, Nc$), Nc is the number of the species (i.e., of the weak acids), C_e is the acid concentration in the bulk phase, C_p is the acid concentration in the adsorbent pores, and q is the concentration of the adsorbed non-dissociated acid remaining in the equilibrium with the concentration of the acid in the eluent contained in the pores.

It is convenient to introduce the following quantities to equation 1: external porosity (bed porosity):

$$\varepsilon_e = \frac{V_e}{V_c} \quad \text{Eq. 2}$$

particle porosity:

$$\varepsilon_p = \frac{V_p}{V_c - V_e} \quad \text{Eq. 3}$$

total porosity:

$$\varepsilon_t = \frac{V_t}{V_c} \quad \text{Eq. 4}$$

After dividing equation 1 by V_c and performing simple algebraic transformations, the following mass balance equation can be obtained:

$$\varepsilon_e \cdot C^{j,HR}_{e,i-1,t-\Delta t} + \varepsilon_e \cdot C^{j,R^-}_{e,i-1,t-\Delta t} + (1-\varepsilon_e)\varepsilon_p \cdot C^{j,HR}_{p,i,t-\Delta t} + \varepsilon_p (1-\varepsilon_e) \cdot C^{j,R^-}_{p,i,t-\Delta t} + (1-\varepsilon_t)\, q^{j,HR}_{i,t-\Delta t} = \varepsilon_t \cdot C^{j,HR}_{i,t} + \left(\varepsilon_e \cdot C^{j,R^-}_{e,i,t} + (1-\varepsilon_e)\varepsilon_p \cdot C^{j,R^-}_{p,i,t} + (1-\varepsilon_t) q^{j,HR}_{i,t}\right) \quad \text{Eq. 5}$$

Equation 5 has to be coupled with the equilibrium isotherm:

$$q^{j,HR} = f(C^{1,HR}, C^{2,HR}, \ldots, C^{Nc,HR}) \quad \text{Eq. 6}$$

and with the equilibrium correlation between the acids and their ions: in the bulk phase (its volume equal to V_e)

$$K^j_a = \frac{C^{R^-,j}_{i,t} \cdot \left(\sum_{r=1}^{Nc} C^{r,R^-}_{e,i,t} + C^{*,R^-}_{e,i,t}\right)}{C^{j,HR}_{i,t}} \quad \text{Eq. 7}$$

for $j = 1, \ldots, Nc$, where K^j_a is the equilibrium dissociation constant of the acid, and C^* denotes the concentration of a strong, monoprotic and completely dissociated acid (if it was present in the system). The generalization for the polyprotic acids is straightforward.

in the eluent occluded in the pores (its volume equal to V_p)

$$K^j_a = \frac{Cj,^{R^-}_{p,i,t} \cdot \left(\sum_{r=1}^{Nc} C^{r,R^-}_{p,i,t} + C^{F^-}_{p,i,t}\right)}{C^{j,HR}_{i,t}} \quad \text{Eq. 8}$$

where C^{F-} is the concentration of the functional group.

The nonlinear algebraic model (5), coupled with equations 6–8, was solved using an iterative method in order to find the concentration of the non-dissociated acid, $C^{j,HR}_{i,t}$ of its dissociated form, and the total concentration.

The time increment was calculated from the relation:

$$\Delta t = \frac{x}{W}$$

where:

$$\Delta x = \frac{L}{N} w = \frac{u}{\varepsilon_e}$$

u is the superficial velocity, and L is the column length. The derived model (equations 5–8) was used for simulations of the separation of acids chromatographed both in the IEC and v-IEC mode. In the former case (IEC), it was assumed that initially (i.e., at $t = 0$) the pure eluent flowed through the column. Then for the time $0 < t \le t_{inj}$, the sample of the weak acid(s) was injected into the column. Immediately thereafter ($t > t_{inj}$), the pure eluent was again delivered to the column inlet.

As previously stated, in the v-IEC mode, a mixture of the analytes was used as the mobile phase, and pure water was injected as the sample (8–12), so that the initial and boundary conditions had to be defined as opposite to those assumed for the IEC technique. At the initial time ($t = 0$), the column was assumed to be filled with the weak acids dissolved in the eluent. A sample of the pure eluent was injected into the column in the time $0 < t \le t_{inj}$, and for $t > t_{inj}$, the eluent containing the weak acids was again delivered to the column inlet.

Experimental

Instrumentation and procedure

Ion separation was performed with use of the Merck-Hitachi (Darmstadt, Germany) LaChrom chromatograph, equipped with the following devices: vacuum degasser L-7612, pump L-7100, column oven L-7350, photodiode array detector DAD L-7455, and an interface D-7000. The IEC and v-IEC experiments were carried out with use of the column filled with the polystyrene–divinylbenzene strongly acidic cation-exchange resin in the H^+ form [Tosoh (Tokyo, Japan) TSKgel SCX (5-µm particle size, pore diameter equal to 60Å, 1.5 mequiv/mL cationic-exchange capacity, 150 m × 6 mm i.d.)]. The experimental conditions were as follows: the column temperature, 25°C; the flow rate, 0.5 mL/min; and the injection volume, 20 µL. The separation column was equilibrated until a stable baseline (the background signal level of the eluent) was obtained. The analytes were detected at the UV wavelength $\lambda = 215$ nm. The retention times for the peak apexes were corrected by subtracting the extra volume dead time (i.e., the time needed by the eluent to flow through the capillaries connecting the valve with the column and the column with the detector) ($t_o = 0.186$ min) from the measured retention times of the peaks in order to obtain the relevant results.

Reagents

All chemicals were of the analytical reagent grade, and they were supplied by Merck KGaA. Standard solutions were prepared without further purification by dissolving the samples in the distilled and deionized water. Needed amounts of the stock solutions of the analytes at the concentration of 0.1M were then diluted with water, as necessary.

IEC

In this study, distilled and deionized water was used as the mobile phase. The standard samples injected into the separation column were the 0.5, 1.0, 2.5, 5.0, 8.0, 16.0, and 32.0mM solutions of the C_1–C_5 carboxylic acids (viz. formic, acetic, propanoic, butanoic, and pentanoic acid).

v-IEC

The 0.5, 1.0, 2.5, 5.0, 8.0, 16.0, and 32.0mM solutions of formic, acetic, propanoic, butanoic, and pentanoic acid were used as the eluents. Each time, the distilled and deionized water was injected into the column as a sample.

Model parameters

The dissociation constants ($pK_{al}^{25°C}$) applied in our calculations for modeling the retention processes in IEC and v-IEC were taken from the literature (23), and they were equal to 3.75, 4.76, 4.86, 4.83, and 4.84 for formic, acetic, propanoic, butanoic, and pentanoic acid, respectively.

The other parameters, indispensable for the solution of the Craig model and expressed in equations 5–8, are the numerical values of total porosity (ε_t) and external porosity (ε_e). They have to be estimated on the basis of the experimental results.

External porosity (ε_e) was calculated for nitric acid from the measured retention time (t_r^{HNO3} = 2.054 min), under the assumption that nitric acid does not penetrate inside the adsorbent particles. It was established that the external porosity amounts to ε_e = 0.242.

Total porosity (ε_t) can be calculated by measuring the retention time of a tracer, which penetrates the adsorbent particles, but does not adsorb on the surface of the pores. The tracer recommended in the literature was methanol. However, from the literature (24) it comes out that when methanol was used as the mobile phase modifier, it slightly lowers the retention time of the adsorptive acids, which most probably can be explained by a weak adsorption of this alcohol on the stationary phase.

In the present study, the aqueous solution of formic acid with the addition of 10mM sulphuric acid was used as a tracer. It was assumed that the non-dissociated molecules of formic acid do not adsorb on the resin. From the experimental retention data of formic acid, eluted by water with an additional low amount of sulphuric acid [as reported in the literature (7)], it was discovered that the retention times of formic acid grow with the increasing concentrations of sulphuric acid. Ultimately, however, when this concentration surpasses (ca. 10mM) they approach a constant value.

The triangular peaks of formic acid, observed when pure water was used as eluent, became Gaussian when sulphuric acid was added to water. The triangular shape was a result of superposition of the ions that migrated faster (after being expelled from the adsorbent) and of the non-dissociated acid molecules (which migrate slower because of their ability to penetrate inside the adsorbent pores). An increased concentration of sulphuric acid in water suppressed the concentration of the acid ions and improved peak symmetry. Finally, for the large enough concentrations of the strong mineral acid in the eluent, the ion concentration of formic acid became negligible, and the peak became Gaussian.

The measured and corrected retention time of formic acid (C = 0.5mM), eluted with the 30mM solution of sulphuric acid, was equal to retention time (t_R) = 5.764 min. This value allowed the estimation of total porosity, which was found as equal to ε_t = 0.679. The particle porosity (ε_p) was calculated from the well known formula:

$$\varepsilon_t = \varepsilon_e + (1 - \varepsilon_e)\varepsilon_p \qquad \text{Eq. 9}$$

The last parameter of the Craig model, which had to be found, was the number of the cells in the column (N). This value was fitted experimentally by obtaining the best correspondence between the experimental and the simulated peak profiles (see the Results and Discussion section).

Results and Discussion

Experimental peak profiles for single analytes in IEC and v-IEC

In Figure 1A, the IEC experimental peak profiles obtained for all the investigated acids in the range of the applied concentrations (i.e., from 0.5 to 32mM) are presented. Pure water was used as the eluent.

In Table I, the retention times of the peak apexes are given. The experimental retention times were corrected by subtracting the extra volume dead time (t_o= 0.186 min) from the measured values.

The retention times of the acids grew with an increasing length of their aliphatic chains because of the hydrophobic interactions with the resin. At the lowest sample concentration (for all investigated acids equal to 0.5mM), the long frontal tailing and a rapid decrease of the concentration at the rear part of the peak (shock) were observed, and the peak concentration profiles resembled the anti-Langmuir peaks. This pattern of the peak profiles was also observed for higher concentrations of the non-adsorbing or very weakly adsorbing species. An explanation of this behavior was simple. The ionized acid particles, expelled from the adsorbent particles, moved faster than the non-dissociated molecules, which could freely penetrate the adsorbent pores. As a result, the anti-Langmuirian concentration profile was formed. It should also be underlined that the retention times of the beginning of a peak for each individual acid did not depend on the concentration of the analyte. On the other hand, the retention times for the rear parts of the peaks of the non-adsorbing or the very weakly adsorbing acids grew with the concentration. Explanation of the latter observation was also simple. For an increasing concentration of the acid sample, the ratio of the non-dissociated form of the acid to the ionized one was growing, as explained by the ther-

modynamic theory of the equilibrium. Consequently, a higher amount of the acid could penetrate inside the pores, and, as a result, with the higher concentrations the rear part of the peak was eluted from the column later than with the lower concentrations. Finally, for the growing concentrations of the acid, a family of the anti-Langmuirian peak profiles, anchored at the same point on the time scale, was observed.

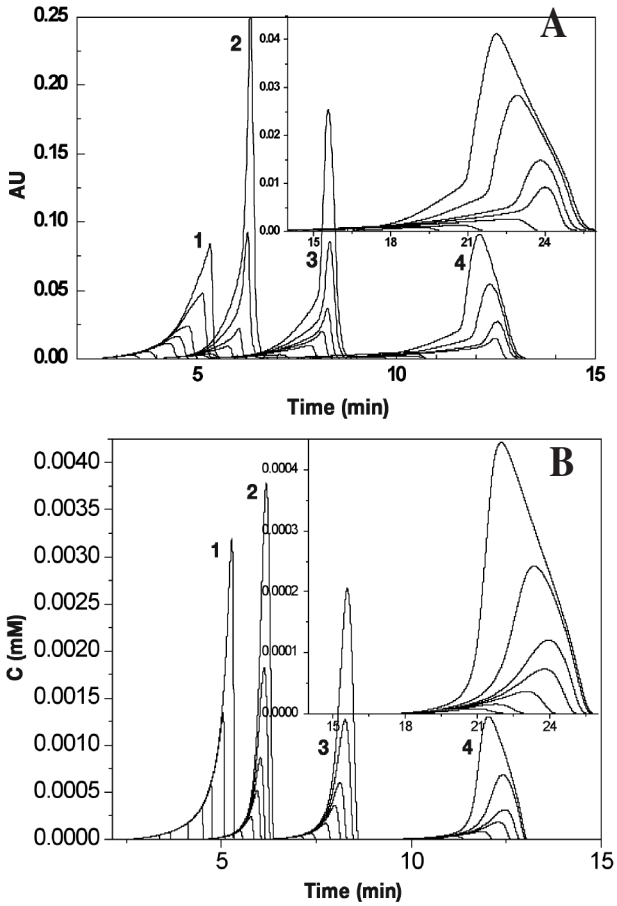

Figure 1. The comparison of the experimental (A) and theoretical (B) concentration profiles on the analysis time in IEC for the following acids: formic, 1; acetic, 2; propanoic, 3; and butanoic, 4; with pentanoic acid in the upper window. Acid concentrations: 0.5, 1, 2.5, 5, 8, 16, and 32mM (from the lowest to the highest peak profile in the series).

The shapes of the peak profiles became more complicated for the more strongly adsorbing acids (to confirm this, please see the peak profiles of pentanoic acid, shown in Figure 1A). With an increased acid concentration, the front tailing slowly disappeared and finally converted to a front shock, whereas the rear shock was slowly converted into a tail. Thus, the peak profiles changed from anti-Langmuirian to Langmuirian. It should also be noticed that the retention times of the peak apexes initially increased with the growing acid concentrations, and they behaved that way up to the analyte concentration in the injected sample of approximately 5mM, and subsequently, they started decreasing. A similar behavior, although less pronounced because of a weaker adsorption, was also observed for butanoic and propanoic acid. Changes in the peak profiles and the apex retention times were a result of the contrary contributions of hydrophobic adsorption and ion exclusion to the distribution of the analyte concentration in the band. As aforementioned, the retention mechanism of pure ion exclusion resulted in the anti-Langmuir shape of the respective peaks. In those cases where retention was governed only by the Langmuir-like adsorption mechanism, the family of the triangular peak profiles (which were mirror reflections of the anti-Langmuir family), could be observed with an increasing concentration of the analyte (19), which is a well recognized fact. The combination of the two mechanisms (i.e., of ion exclusion and adsorption) was responsible for the observed change of the peak profiles from the anti-Langmuir to the Langmuir-like.

The analogous retention behavior was observed with the acids in the ν-IEC experiments. The three exemplary sets of peak profiles for formic, propanoic, and pentanoic acid are shown in Figures 2A, 3A, and 4A. The front tailing effect seen in ν-IEC was much less pronounced than in the classical IEC. The retention times of the peak apexes for all the investigated acids and the applied sample concentrations are given in Table II. With formic acid, the retention time increased with the concentration growth, whereas with butanoic and pentanoic acid the opposite regularity was observed, namely the retention time decreased with the increase in concentration. A more complicated behavior

Table I. Comparison of the Experimental and the Theoretical Retention Times (t_R) of the Peak Apexes in IEC with Pure Water used as Eluent

	Acid														
	Formic			Acetic			Propanoic			Butanoic			Pentanoic		
	t_R (min)			t_R (min)			t_R (min)			t_R (min)			t_R (min)		
C (mM)	Exp.	Theor.	Δt (%)	Exp.	Theor.	Δt (%)	Exp.	Theor.	Δt (%)	Exp.	Theor.	Δt (%)	Exp.	Theor.	Δt (%)
0.5	3.34	3.34	0.00	5.12	5.25	2.54	6.41	7.05	9.98	9.41	10.63	12.9	19.02	20.87	9.73
1	3.78	3.62	4.23	5.32	5.48	3.01	7.05	7.35	4.25	10.30	11.14	8.15	20.77	21.27	2.41
2.5	4.26	4.11	3.52	5.76	5.74	0.35	7.81	7.73	1.02	11.78	11.85	0.59	22.69	23.06	1.63
5	4.49	4.48	0.22	6.04	5.93	1.82	8.12	7.98	1.72	12.46	12.29	1.36	24.00	23.76	1.00
8	4.76	4.73	0.63	–	6.02	–	8.25	8.11	1.69	12.50	12.45	0.40	23.80	23.90	0.42
16	5.10	5.05	0.98	6.25	6.11	2.24	8.32	8.25	0.84	12.33	12.40	0.57	22.93	23.33	1.74
32	5.32	5.28	0.75	6.33	6.17	2.53	8.28	8.29	0.12	12.06	12.02	0.33	22.09	21.95	0.64

was noticed with propanoic acid. In this case, the retention time grew with the increase of the analyte concentration to a certain value, and then a decrease of the retention time was observed, accompanying a further increase of concentration of the analyte in the eluent.

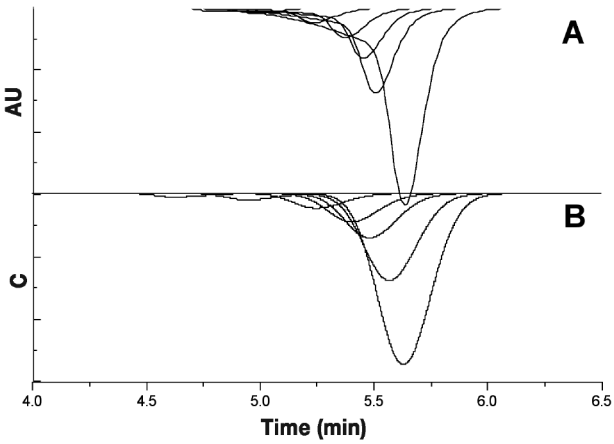

Figure 2. The comparison of the experimental (A) and theoretical (B) concentration profiles of formic acid, analyzed in the v-IEC mode. Acid concentrations: 0.5, 1, 2.5, 5, 8, 16, and 32mM (from left to right).

The experimental v-IEC results can be explained by the mixed mechanism of the acid ions' exclusion and the hydrophobic adsorption of the non-dissociated acid molecules in the same way, as was the case with IEC. For formic acid, with the sole ion-exclusion mechanism available in its case, the growth of the acid concentration was accompanied by the shift of the respective peak profiles to the right because of the increasing ratio of the non-dissociated to the dissociated acid molecules. With butanoic and pentanoic acid, the adsorption mechanism prevailed over ion exclusion, and the peaks were shifted to the left with the concentration growth. This behavior is well know from the literature as Langmuirian adsorption (19). Finally, in the intermediate case of propanoic acid, the increase, followed by the later decrease of the retention time with the increasing acid concentration could be expected.

Theoretical peak profiles for single analytes in IEC and v-IEC

The band profiles obtained by means of IEC and v-IEC were

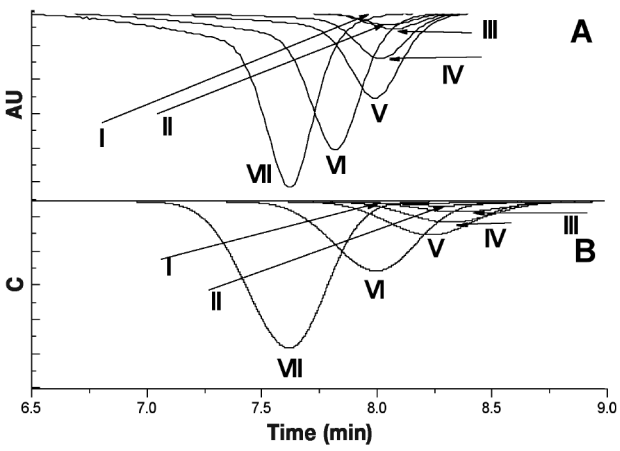

Figure 3. The comparison of the experimental (A) and theoretical (B) concentration profiles of propanoic acid, analyzed in the v-IEC mode. Acid concentration: 0.5 (I), 1 (II), 2.5 (III), 5 (IV), 8 (V), 16 (VI), and 32mM (VII).

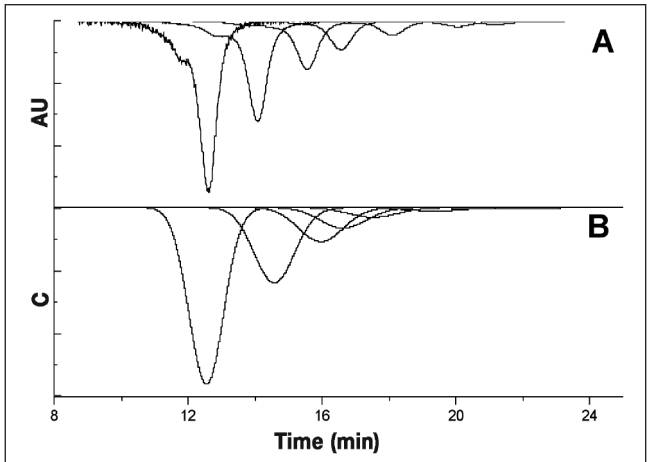

Figure 4. The comparison of the experimental (A) and theoretical (B) concentration profiles of pentanoic acid, analyzed in the v-IEC mode. Acid concentrations: 0.5, 1; 1, 2; 2.5, 3; 5, 4; 8, 5; 16, 6; and 32mM, 7 (from right to left).

Table II. Comparison of the Experimental and the Theoretical Retention Times (t_R) of the Peak Apexes in v-IEC*

	Acid														
	Formic			Acetic			Propanoic			Butanoic			Pentanoic		
	t_R (min)			t_R (min)			t_R (min)			t_R (min)			t_R (min)		
C (mM)	Exp.	Theor.	Δt (%)	Exp.	Theor.	Δt (%)	Exp.	Theor.	Δt (%)	Exp.	Theor.	Δt (%)	Exp.	Theor.	Δt (%)
0.5	4.80	4.62	3.75	5.93	5.97	0.67	7.94	8.14	2.51	11.94	12.62	5.69	21.18	21.44	1.23
1	4.97	4.94	0.60	6.03	6.08	0.83	8.05	8.29	2.98	11.80	12.27	3.98	20.07	19.34	3.64
2.5	5.22	5.24	0.38	6.13	6.17	0.65	8.07	8.35	3.46	11.37	11.34	0.26	18.08	17.49	3.26
5	5.37	5.40	0.56	6.17	6.20	0.49	8.01	8.31	3.74	10.97	10.61	3.28	16.57	16.61	0.24
8	5.44	5.48	0.73	6.19	6.20	0.16	7.99	8.22	2.88	10.63	10.22	3.86	15.56	15.94	2.44
16	5.50	5.56	1.09	6.20	6.17	0.48	7.81	7.99	2.30	10.05	9.81	2.39	14.07	14.55	3.41
32	5.62	5.62	0	6.20	6.12	1.29	7.62	7.61	0.13	9.45	9.42	0.32	12.60	12.52	0.63

* Water with the specified concentration (C) of the given acid was used as the eluent.

modeled using the Craig method (equations 5–8). It was assumed that the adsorption of the non-dissociated molecules of formic acid was negligible. However, the role of adsorption in the retention of the other acids was considerable. Initially, the pH value of water in volume (V_e) was assumed as equal to 7. Unfortunately, this assumption led to discrepancies between the calculated and the experimental results. Namely, for C = 0.5mM, the calculated retention time of formic acid was equal to 3.12 min, whereas the experimental retention time was equal to 3.34 min. Moreover, the calculated peak profiles for pentanoic acid always began after approximately 2.1 min from the start of the analysis, regardless of the concentration and the assumed adsorption mechanism, whereas the experimental peak profiles of pentanoic acid emerged after 15 min from the injection only. Thus, it was concluded that the adsorption on the external surface of the adsorbent particles alone cannot explain the peak retardation because of a very small external surface area (lower than 1 m^2 per gram of the adsorbent).

In this work, a strongly acidic cation-exchange resin with 1.5 mequiv/mL cationic-exchange capacity was used. Thus, the concentration of the H^+ ions in the resin pores was equal to 1.5M. The functional groups were located on the external surface of the resin also, so that the H^+ ions originating from these functional groups penetrate the water percolating among the resin particles. Therefore, an average concentration of the H^+ ions should be higher than 10^{-7} [and, consequently, that the assumed pH of water in the volume (V_e) should be lower than 7]. This particular doubt and a resulting conclusion led to a more realistic average concentration of the H^+ ions assumed in this study and, hence, to a remarkably better agreement between the experimental and the theoretical results, which are now going to be discussed.

An apparent concentration of the hydrogen ions in mobile water can be calculated by the estimation of the concentration (C^*) in equation 7 in such a way as to obtain the calculated retention time of formic acid at C = 0.5mM, equal to the experimental retention time of 3.34 min. The estimated value of C^* (equal to 2×10^{-5}mM) was then used for the simulation of the peak profiles of formic acid, chromatographed by means of IEC and ν-IEC for all sample concentrations. The obtained peak profiles and the calculated retention times of the peak apexes remain in good agreement with the experiment (see Figures 1A and 1B, and Tables I and II). The relative error:

$$\Delta t = \frac{|t_{exp} - t_{theor}|}{t_{exp}} \cdot 100\% \qquad \text{Eq. 10}$$

of calculation of the retention time was less than 1% for almost all the experiments with formic acid. In all the theoretical simulations performed for the other acids considered in this study, the value of $C^* = 2 \times 10^{-5}$mM was then applied.

As previously described, the retention of the acids increased with the growing length of the aliphatic moiety in the acid molecule because of its hydrophobic interactions with the resin. Therefore, it was assumed that the non-dissociated acid molecules could penetrate inside the resin and adsorb on the surface of the pores. In the first instance, the simple Langmuirian model was applied. With this particular isotherm it proved, however, rather impossible to model the effect of the increasing and decreasing retention times of the peak apexes within the assumed range of the acid concentrations. Only after the assumption that at least two different active sites exist on the resin skeleton, was a correct prediction of the dependency between the retention times and the inlet concentrations of the analyte samples possible. In the following, the bi-Langmuirian isotherm, given below, was used:

$$q = \frac{q_{s1}K_1C}{1 + K_1C} + \frac{q_{s2}K_2C}{1 + K_2C} \qquad \text{Eq. 11}$$

where q_{s1} and q_{s2} are the saturation capacities of the active sites, and K_1 and K_2 are the appropriate equilibrium constants.

The parameters of the bi-Langmuir model and the number of cells in the Craig model were estimated using the inverse method (i.e., by obtaining of the best available agreement between the experimental and the theoretical peak profiles) and also by obtaining the best agreement between the experimental and the theoretical retention times of the peak apexes. Estimation was performed jointly for the IEC and the ν-IEC peaks obtained for the highest sample concentration, equal to 32mM. The calculated parameters of the model are summarized in Table III. As demonstrated in these data, the saturation capacities for both active sites did not change remarkably for different acids; however, the equilibrium constant (the energy of interactions between the acid and the skeleton of the resin), especially for the high energy active sites (second sites), increased rapidly with the increase of the aliphatic chain length. It is also evident from the data given in Table III that the number of cells required for the best approximation of the experimental peak profiles decreases with the increasing aliphatic chain length, which means the mass transfer resistances increased for higher acids. A detailed investigation of the mass transfer resistances was, however, beyond the scope of this paper.

The estimated parameter values of the bi-Langmuir isotherm were used for simulation of the peak profiles for all the investigated acids, with the sample concentrations ranging from 0.5 to 32mM, both in the IEC and the ν-IEC modes. The theoretical peak profiles originating from IEC are shown in Figure 1B, and they correspond well with the experimental bands given in Figure 1A. Figures 2B, 3B, and 4B show the typical vacancy concentration profiles originating from our calculations. All of the vacancy profiles were tuned to the equal concentration level in order to mimic the detector signal. The peak shapes and the peaks depths were not changed. It was very easy to notice that the Craig model predicted the disappearance of the front tailing

Table III. Numerical Values of the Bi-Langmuir Isotherm Model Coefficients*

Acid	q_{s1}	K_1	q_{s2}	K_2	N
Formic	–	–	–	–	1500
Acetic	0.1437	0.6869	0.0059	21.97	1500
Propanoic	0.1374	5.712	0.01428	20.93	1500
Butanoic	0.5453	2.93	0.005723	281	1000
Pentanoic	0.4136	10.81	0.00364	1385	500

* N is the number of theoretical cells used in the performed simulations.

in the v-IEC mode in a correct manner.

A comparison of the experimental and the theoretical retention times of the peak apexes for all sample concentrations is given in Tables I (IEC) and II (v-IEC). Additionally, these tables presented the relative error of calculation of the retention times for all acids. As shown, the error of the retention time prediction was sporadically higher than 5%, and it was less than 2% for approximately 60% of the experiments.

The proposed model accurately predicted qualitative and quantitative changes of the retention time as a function of the analytes' concentration for all the investigated compounds chromatographed by means of IEC and v-IEC.

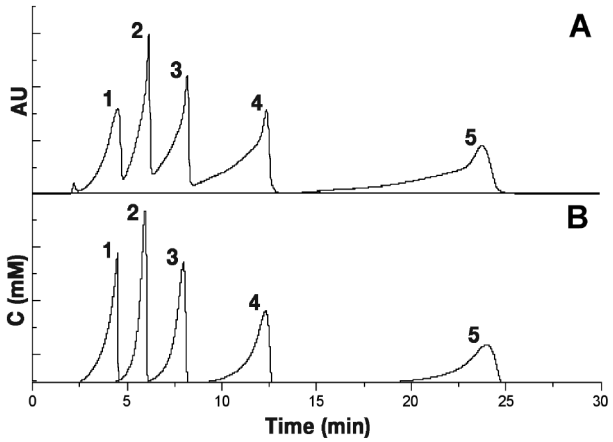

Figure 5. The comparison of the experimental (A) and theoretical (B) concentration profiles for the 5mM solutions of: formic, 1; acetic, 2; propanoic, 3; butanoic, 4; and pentanoic acid, 5, eluted with pure water in the IEC mode. Theoretical calculations were performed for $N = 1000$.

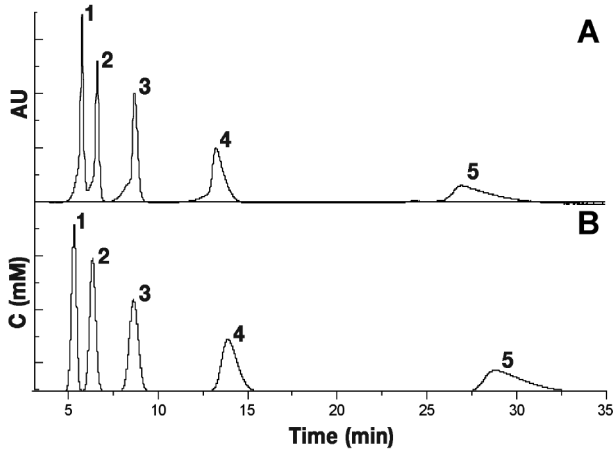

Figure 6. The comparison of the experimental (A) and the theoretical (B) concentration profiles for the 5mM solutions of formic, 1; acetic, 2; propanoic, 3; butanoic, 4; and pentanoic acid, 5, eluted with the 1mM aqueous solution of H_2SO_4 in the IEC mode. Theoretical calculations were performed for $N = 1000$.

Retention of single analytes in IEC with the 1mM aqueous solution of sulphuric acid as eluent

In the IEC experiments, it is a common practice to use water with a low concentration of a strong mineral acid (e.g., sulphuric acid) as the mobile phase. The strong acid suppresses dissociation, thus increasing the amount of the non-dissociated acid molecules, which resulted in a reduced frontal tailing in an increased retention time and, hence, in an improved separation of the species. The main drawback of this method was an increased time of running the analysis and a greater back-tailing of the strongly adsorptive acids, which was particularly evident when applying the concentration overload conditions. The discussed feature of elution in presence of a strong mineral acid is well depicted in the case of the multicomponent IEC analysis (see Figures 5A and 6A).

The Craig model previously proposed (see the Craig model of IEC and v-IEC section) takes into account the presence of the considerably diluted strong acid, thus enabling direct calculation of the retention of the weak acids. Specifically, the numerical value of the concentration of sulphuric acid (C^*) multiplied by two (because sulphuric acid is a divalent acid) had to be introduced in equation 7. The remaining model parameters were the same as those described in the Theoretical peak profiles for single analytes in the IEC and v-IEC section.

In Table IV, a comparison of the experimental with the calculated retention times of the peak apexes is given for the acids developed separately. The relative error of the retention time calculations was generally equal to approximately 1–2%. Only for formic acid did it increased to almost 7%.

Retention of multicomponent samples in the IEC and v-IEC mode

In Figure 5A, the separation of all the acids investigated in this study is presented by means of IEC and using pure water as the mobile phase. In Figure 6A, the analogous separation achieved by means of the 1mM aqueous solution of sulphuric acid as the eluent was given. Simulated separation of the acids in each of the

Table IV. Comparison of the Experimental and Theoretical Retention Times (t_R) of the Peak Apexes in IEC with the 1mM Solution of H_2SO_4 used as Eluent

	Acid														
	Formic			Acetic			Propanoic			Butanoic			Pentanoic		
	t_R (min)			t_R (min)			t_R (min)			t_R (min)			t_R (min)		
C (mM)	Exp.	Theor.	Δt (%)	Exp.	Theor.	Δt (%)	Exp.	Theor.	Δt (%)	Exp.	Theor.	Δt (%)	Exp.	Theor.	Δt (%)
0.5	5.60	5.22	6.78	6.47	6.32	2.32	8.84	8.63	2.37	14.48	14.26	1.52	32.78	30.91	5.70
5	5.63	5.29	6.04	6.45	6.31	2.17	8.72	8.62	1.15	13.72	13.89	1.24	28.96	29.24	0.97

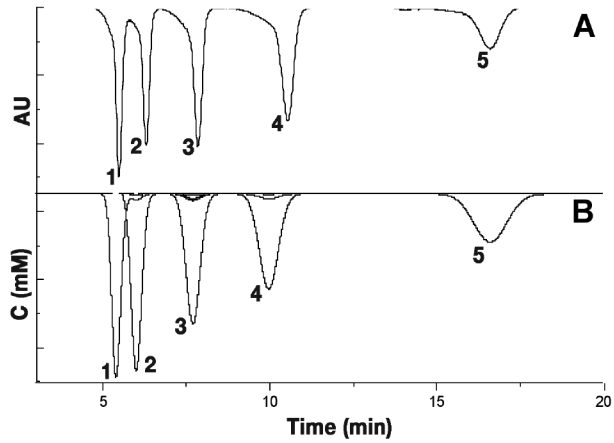

Figure 7. The comparison of the experimental (A) and theoretical (B) concentration profiles for the 5mM solutions of formic, 1; acetic, 2; propanoic, 3; butanoic, 4; and pentanoic acid, 5, eluted with pure water in the v-IEC mode. Theoretical calculations were performed for $N = 1000$.

two cases considered is given in Figures 5B and 6B. In these simulations, the multicomponent bi-Langmuir model was applied. In spite of the fact that the multicomponent bi-Langmuir isotherm was thermodynamically inconsistent (because of the different saturation capacities for the different acids), the predicted separation of the acids remained in good agreement with the experiment. The relative error of calculation of the retention times of peak apexes was less than 3% when pure water was used as the eluent, and it was contained between 0.5% and 8% when the aqueous solution of sulphuric acid was applied. A similar agreement between the observed and the simulated separation of the investigated acids by means of v-IEC (see Figures 7A and 7B) was obtained. The maximum relative error of the calculated retention time was less than 5.5%. The additional small peaks visible in Figure 7B are the so-called system peaks, predicted by the theory of Helfferich and Klein (19,25) for the nonlinear adsorption. However, these peaks cannot be separately measured with the aid of the UV detector applied in this study.

Conclusion

In this investigation, a simple Craig model, coupled with the relationship describing the equilibrium between the non-dissociated acid molecules and the ions thereof, and additionally implemented by the bi-Langmuir adsorption isotherm model, was used for the prediction of the retention of the nonadsorptive and adsorptive organic acids in IEC and in v-IEC mode. The model was successfully verified with the aid of a strongly acidic ion-exchange resin in the H^+-form, characterized by the small pore diameter, equal to 60 Å. It turned out that the retention values and the peak shapes, predicted using the newly devised equations, are well confirmed by the experimental results.

These equations enable the prediction of certain new features, characteristic of IEC and v-IEC, which were confirmed experimentally. The results indicated that in the IEC mode, the retention times of the peak apexes for the adsorptive acids increased up to a certain level with the growth of their respective concentrations, and then the retention times started decreasing with the further increase of the analyte concentration. In v-IEC of the nonadsorptive acids, the retention times of the peak apexes increase with the growth of the acid concentration, whereas with the adsorptive acids, the increase of their concentration in the injected samples was accompanied by the decrease of the respective retention times. Moreover, with the aid of the applied model, the disappearance of the frontal peak tailing in v-IEC and also in IEC can be predicted, when the 1mM aqueous solution of sulphuric acid is used as the eluent. The calculated and the experimental retention times of the peak apexes and the predicted and the experimental elution profiles remain in a good mutual agreement for a wide range of the concentrations with all the analytes investigated in this study.

Finally, the model was successfully applied to the prediction of the separation effect with a multicomponent mixture of the weak acids, when pure water (IEC and v-IEC), and also water with a low concentration of the strong mineral acid (IEC), were used as the eluent.

Acknowledgments

The authors wish to express their grateful appreciation to Professor Kazuhiko Tanaka (National Institute of AIST, Seto, Japan) for kindly providing us with the Tosoh TSKgel SCX column, which enabled the experimental verification of the model. Also, Merck KGaA is thankfully acknowledged for supplying the chemicals for the experiments.

References

1. B.K. Glód. Ion exclusion chromatography: parameters influencing retention. *Neurochem. Res.* **22:** 1237–48 (1997).
2. B.K. Glód. Indirect detection in ion-exclusion chromatography. *Acta Chromatogr.* **12:** 122–28 (2002).
3. K. Tanaka and J.S. Fritz. Separation of aliphatic carboxylic acids by ion-exclusion chromatography using a weak-acid eluent. *J. Chromatogr.* **361:** 151–60 (1986).
4. K. Tanaka, M. Mori, Q. Xu, M.I.H. Helaleh, M. Ikedo, H. Taoda, W. Hu, K. Hasebe, J.S. Fritz, and P.R. Haddad. Ion-exclusion chromatography with conductimetric detection of aliphatic carboxylic acids on a weakly acidic cation-exchange resin by elution with benzoic acid–β-cyclodextrin. *J. Chromatogr. A* **997:** 127–32 (2003).
5. K. Ito, Y. Takayama, M. Ikedo, M. Mori, H. Taoda, Q. Xu, W. Hu, H. Sunahara, T.Hayashi, S. Sato, T. Hirokawa, and K. Tanaka. Determination of some aliphatic carboxylic acids in anaerobic digestion process waters by ion-exclusion chromatography with conductimetric detection on a weakly acidic cation-exchange resin column. *J. Chromatogr. A* **1039:** 141–45 (2004).
6. B. Glód and W. Kemula. Separation mechanism and determination of acidic compounds by ion-exclusion liquid chromatography with elektrokinetic detection. *J. Chromatogr.* **366:** 39–50 (1986).
7. K. Tanaka, H. Chikara, W. Hu, and K. Hasebe. Separation of carboxylic acids on a weakly acidic cation-exchange resin by ion-exclusion chromatography. *J. Chromatogr. A* **850:** 187–196 (1999).
8. K. Tanaka, M.-Y. Ding, M.I.H. Helaleh, H. Taoda, H. Takahashi, W. Hu, K. Hasebe, P.R. Haddad, J.S. Fritz, and C. Sarzanini. Vacancy ion-exclusion chromatography of carboxylic acids on a

weakly acidic cation-exchange resin. *J. Chromatogr. A* **956:** 209–14 (2002).
9. K. Tanaka, M.-Y. Ding, H. Takahashi, M. I. H. Helaleh, H. Taoda, W. Hu, K. Hasebe, P.R. Haddad, M. Mori, J.S. Fritz, and C. Sarzanini. Vacancy ion-exclusion chromatography of carboxylic acids on a strongly acidic cation-exchange resin. *Anal. Chim. Acta* **474:** 31–35 (2002).
10. M.I.H. Helaleh, K. Tanaka, M. Mori, Q. Xu, H. Taoda, M.-Y. Ding, W. Hu, K. Hasebe, and P.R. Haddad. Vacancy ion-exclusion chromatography of haloacetic acids on a weakly acidic cation-exchange resin. *J. Chromatogr. A* **997:** 133–38 (2003).
11. M.I.H. Helaleh, K. Tanaka, M. Mori, Q. Xu, H. Taoda, M.-Y. Ding, W. Hu, K. Hasebe, and P.R. Haddad. Vacancy ion-exclusion chromatography of aromatic carboxylic acids on a weakly acidic cation-exchange resin. *J. Chromatogr. A* **997:** 139–44 (2003).
12. M. Mori, M.I.H. Helaleh, Q. Xu, W. Hu, M. Ikedo, H. Taoda, and K. Tanaka. Vacancy ion-exclusion/adsorption chromato-graphy of aliphatic amines on a polymethacrylate-based weakly basic anion-exchange column. *J. Chromatogr. A* **1039:** 129–33 (2004).
13. M.I.H. Helaleh, K. Tanaka, M. Mori, Q. Xu, H. Taoda, M.-Y. Ding, W. Hu, K. Hasebe, and P.R. Haddad. Vacancy ion-exclusion chromatography of aromatic carboxylic acids on a weakly acidic cation-exchange resin. *J. Chromatogr. A* **997:** 139–44 (2003).
14. K. Tanaka, M.-Y. Ding, H. Takahashi, M.I.H. Helaleh, H. Taoda, W. Hu, K. Hasebe, P.R.Haddad, M. Mori, J.S. Fritz, and C. Sarzanini. Vacancy ion-exclusion chromatography of carboxylic acids on a strongly acidic cation-exchange resin. *Anal. Chim. Acta* **474:** 31–35 (2002).
15. K. Tanaka, M.-Y. Ding, M.I.H. Helaleh, H. Taoda, H. Takahashi, W. Hu, K. Hasebe, P.R. Haddad, J.R. Fritz, and C. Sarzanini. Vacancy ion-exclusion chromatography of carboxylic acids on a weakly acidic cation exchange resin. *J. Chromatogr. A* **956:** 209–14 (2002).
16. B.K. Glód, A. Piasecki, and J. Stafiej. Numerical simulation of column performance in ion-exclusion chromatography. *J. Chromatogr.* **457:** 43–53 (1988).
17. B.K. Glód, A. Piasecki, and J. Stafiej. Model for the mixed ion-exclusion-adsorption retention mechanism in ion-exclusion chromatography. *J. Chromatogr.* **654:** 197–205 (1993).
18. K. Kaczmarski, M. Mori, B. Glód, T. Kowalska, and K. Tanaka. Modeling of ion-exclusion and vacancy ion-exclusion chromatography on a strongly acidic cation-exchange resin in the H+ form. *Acta Chromatogr.* **15:** 66–81 (2005).
19. G. Guiochon, S. Golshan-Shirazi, and A.M. Katti. *Fundamentals of Preparative and Nonlinear Chromatography*. Academic Press, Boston, MA, 1994.
20. D.M. Ruthven. *Principles of Adsorption & Adsorption Processes*. John Wiley & Sons, New York, NY, 1984.
21. B.K. Glód, A. Piasecki, and J. Stafiej. Numerical simulation of column performance in ion-exclusion chromatography. *J. Chromatogr.* **457:** 43–53 (1988).
22. K. Kaczmarski and D. Antos. Calculation of chromatographic band profiles with an implicit isotherm. *J. Chromatogr. A* **862:** 1–16 (1999).
23. ZirChrom Separations Inc. Dissociation constants of organic acids and bases. http://www.zirchrom.com/organic.htm (accessed Oct. 2005).
24. K. Ohta, A. Towata, and M. Ohashi. Ion-exclusion chromatographic behavior of aliphatic carboxylic acids and benzenecarboxylic acids on a sulfonated styrene-divinyl-benzene co-polymer resin column with sulfuric acid containing various alcohols as eluent. *J. Chromatogr. A* **997:** 95–106 (2003).
25. F. Helfferich and G. Klein. *Multicomponent Chromatography. A Theory of Interferences.* M. Dekker, New York, NY, 1970.

Manuscript received October 27, 2005;
revision received May 8, 2006.